REPORT DOCUMENTATION PAGE

Form Approved
OMB No. 0704-0188

PLEASE DO NOT RETURN YOUR FORM TO THE ABOVE ADDRESS.

1. REPORT DATE *(DD-MM-YYYY)*	2. REPORT TYPE	3. DATES COVERED *(From - To)*
JULY 2009	Technical Paper Post Print	June 2008 – August 2008

4. TITLE AND SUBTITLE

A MIMO-INSPIRED RAPIDLY SWITCHABLE PHOTONIC INTERCONNECT ARCHITECTURE

5a. CONTRACT NUMBER
In House

5b. GRANT NUMBER
N/A

5c. PROGRAM ELEMENT NUMBER
62702F

6. AUTHOR(S)

Henry Zmuda, Joseph Osman, Michael Fanto, Thomas McEwen

5d. PROJECT NUMBER
OPIS

5e. TASK NUMBER
00

5f. WORK UNIT NUMBER
00

7. PERFORMING ORGANIZATION NAME(S) AND ADDRESS(ES)

University of Florida, Dept of Electrical & Computer Engineering, Gainsville, FL
Air Force Research Laboratory (AFRL) 525 Brooks Road, Rome, NY 13441

8. PERFORMING ORGANIZATION REPORT NUMBER
N/A

9. SPONSORING/MONITORING AGENCY NAME(S) AND ADDRESS(ES)

AFRL/RISC
525 Brooks Road
Rome NY 13441-4505

10. SPONSOR/MONITOR'S ACRONYM(S)
N/A

11. SPONSORING/MONITORING AGENCY REPORT NUMBER
AFRL-RI-RS-TP-2009-12

12. DISTRIBUTION AVAILABILITY STATEMENT

Approved for public release; distribution unlimited. PA# 88ABW-2009-1292 Date Cleared: 3-April-2009

13. SUPPLEMENTARY NOTES

14. ABSTRACT

It is well-known that interconnect issues pose a significant bottleneck with regard to improving the performance of high-speed integrated systems such as a cluster of computer processing units. Power, speed (bandwidth), and size all affect the computational performance and capabilities of future systems. Highspeed optical processing has been looked to as a means for eliminating this interconnect bottleneck. Presented here are the results of a study for a novel optical (integrated photonic) processor which would allow for a high-speed, secure means for arbitrarily addressing a multiprocessor system. This paper will present analysis, simulation, and optimization results for the architecture as well as considerations for a
proof-of-concept level system design. The architecture takes advantage of spatial and wavelength diversity and in this regard may be regarded as a Multiple Input Multiple Output (MIMO) architecture.

15. SUBJECT TERMS

Free-space optical interconnects, Optical Phased Arrays, High-Speed Optical Beamsteering, Optical MIMO, Microwave Photonics

16. SECURITY CLASSIFICATION OF:			17. LIMITATION OF ABSTRACT	18. NUMBER OF PAGES	19a. NAME OF RESPONSIBLE PERSON
					Joseph Osman
a. REPORT	b. ABSTRACT	c. THIS PAGE			19b. TELEPHONE NUMBER (*Include area code*)
U	U	U	UU	10	N/A

A MIMO-INSPIRED RAPIDLY SWITCHABLE PHOTONICINTERCONNECT ARCHITECTURE

Henry Zmuda
University of Florida
Department of Electrical and Computer Engineering
Gainesville, FL

Joseph Osman, Michael Fanto and **Thomas McEwen**
Air Force Research Laboratory, Information Directorate
Rome, NY

ABSTRACT

It is well-known that interconnect issues pose a significant bottleneck with regard to improving the performance of high-speed integrated systems such as a cluster of computer processing units. Power, speed (bandwidth), and size all affect the computational performance and capabilities of future systems. High-speed optical processing has been looked to as a means for eliminating this interconnect bottleneck. Presented here are the results of a study for a novel optical (integrated photonic) processor which would allow for a high-speed, secure means for arbitrarily addressing a multiprocessor system. This paper will present analysis, simulation, and optimization results for the architecture as well as considerations for a proof-of-concept level system design. The architecture takes advantage of spatial and wavelength diversity and in this regard may be regarded as a Multiple Input Multiple Output (MIMO) architecture.

A given node to be addressed, rather than having a wired metal contact as an output, has as a radiating laser source that has been modulated with the data to be conveyed to another point in the system. Each processor node radiates a different optical wavelength. Each individual wavelength is chosen, for example, to correspond to the wavelengths associated with a WDM ITU grid. All wavelengths are incident on a coherent fiber bundle which acts as an array receiver. Unlike conventional phased arrays, the receive elements are spaced many wavelengths apart giving rise to a large number of grating lobes. It will be shown that by using appropriate photonic/optical signal processing methods any node of the processor cluster can be randomly and rapidly addressed using high-speed phase shifters (electrooptic or others) as control elements. The diversity techniques employed achieve high gain and a narrow beamwidth in the direction of the desired node and high attenuation with regard to the signals from all other nodes. As is often the case of MIMO-bases systems, overall performance exceeds that of diffraction limited array processing.

In addition to the interconnect application discussed, the methods described in this paper can also be applied to other applications where rapid electrical (non-mechanical) optical beamsteering is required such as raster scanned laser radar systems and tracking, guidance, and navigation systems.

KEYWORDS: Free-space optical interconnects, Optical Phased Arrays, High-Speed Optical Beamsteering, Optical MIMO, Microwave Photonics

1 INTRODUCTION

1.1 Optical Phased Arrays

The ability of phased array antennas for beam steering application are well known, and system designers have searched for ways to transition these benefits to optically-based systems [1–3]. Though many similarities exist between optical and RF/microwave beamforming systems there exist significant

Enabling Photonics Technologies for Defense, Security, and Aerospace Applications V,
edited by Michael J. Hayduk, Peter J. Delfyett Jr., Andrew R. Pirich, Eric J. Donkor, Proc. of SPIE Vol. 7339,
73390K · © 2009 SPIE · CCC code: 0277-786X/09/$18 · doi: 10.1117/12.822116

differences as well. RF phased array antennas can provide, in theory, a diffraction limited beam on-target with a 3-dB beamwidth on the order of λ/Nd, where λ is the RF carrier center wavelength, d is the array element spacing, and N is the number of radiating elements. Through coherent addition of fields, the power on-target is proportional to N^2P_o where P_o is the power radiated by each element. Further, and perhaps most significantly, the antenna pattern for a phased array antenna can be steered (scanned) electronically as well as shaped, which, for the case of a narrow RF bandwidth, is accomplished simply by means of phase and amplitude control of the carrier signal at each radiating element. Electronic scanning of the beam allows for a rapidly reconfigurable far-field beampattern without physical motion of the antenna. These last two features, namely the directional gain and non-mechanical beam pointing, are obviously attractive for optical beam steering systems as well.

These benefits of *RF* array beamforming techniques are mitigated however when one considers the practical limitations imposed by a phased array system operating at an optical carrier. Since the individual lasers are generally not coherent, the power for N lasers increases by a factor N as compared to N^2 for coherent radiators. More significantly, the lack of coherence among the laser sources prevents the use of array beamforming methods in the fullest sense. Consequently non-electronic steering of the beam, mechanical or otherwise, is still required. Even with an array of coherent (phase-locked) laser sources, coherent beamforming is still poses problems. This is because conventional beamforming techniques require that the inter-element array spacing be at most equal to one-half the operational wavelength or $d \leq \lambda/2$. For practical systems with an operating wavelength on the order of 1 – 2 microns, such spacing is impossible. Indeed, the core diameter alone of a single-mode optical fiber is on the order of several microns and several tens of microns for a multi-mode fiber. Array element spacing on the order of many wavelengths results in the production grating lobes, where energy is radiated in many directions and gives rise to spatial ambiguity.

These considerations unfortunately have made conventional array beamforming techniques effectively impractical for optical applications. The sought after array advantage of increased power and electronic steering capability applied to optical systems requires a new paradigm which is introduced in the section to follow.

1.2 MIMO-Based Optical Phased Arrays

This paper examines the use of MIMO techniques to achieve optical beamsteering. MIMO radar techniques have been motivated by recent advances in communication theory. It has been shown that unlike a conventional phased array which transmits appropriately weighted, delayed (or phase-shifted) versions of the *same* signal, a MIMO array transmits *multiple* signals that are, in general, quite different from each other. This difference, termed waveform diversity, forms the essence of MIMO arrays, and enables superior capabilities compared with standard phased-array radar technology [4–8]. For example, for either co-located or bi-static transmit and receive antennas, MIMO radar has been shown to offer higher resolution [4] and sensitivity (to detecting slowly moving targets) [5], better parameter identifiably [6], and direct applicability of adaptive array techniques [7, 8]. In the field of communications MIMO approaches have been shown to improve the bit error rate in a communications channel beyond that of the Nyquist limit. Here too will the techniques presented allow for beam resolution which far exceeds the diffraction limit of the N-element aperture.

2 THEORY OF OPERATION

2.1 General MIMO Array Topology

Figure 1 illustrates the MIMO concept in conceptual form. The M radiating sources transmit *independent* signals $x_0, \cdots, x_{M-1}$. These signals are detected by N receive elements $y_0, \cdots, y_{N-1}$. Note that a particular receive element, say y_n, receives M weighted independent signals $\alpha_{n,0}x_0, \cdots, \alpha_{n,M-1}x_{M-1}$, where the coefficients $\alpha_{m,n}$ account for the propagation effects from transmit element m to receive element n.

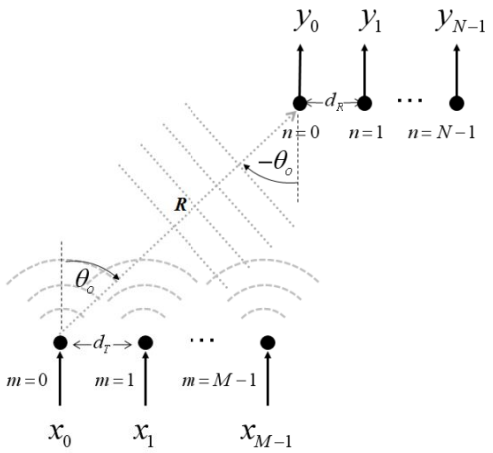

Figure 1: Conceptual illustration of a MIMO-bases array architecture. Assumed here is a Uniform Linear Array (ULA) Topological architecture for an *M*-element-transmit and *N*-element-receive MIMO array with the receiver assumed to be in the far-field of the transmitter.

Consider the case of a uniform linear array (ULA) for both the transmitter and receiver, as shown in Figure 1. The radiating elements are spaced by a distance d_T while the receiver elements are spaced by d_R. It is assumed that both d_T and d_R are much greater than the usual half-wavelength spacing. Examination of Figure 1 shows, that with the usual far-field approximations, a signal (electric or magnetic field) $x_m(t)$ emanating from the m^{th} radiator and upon reception at the n^{th} receiver element will be of the form,

$$y_{m,n}(t) = \alpha_{m,n} x_m\left(t - T_{m,n}\right) \tag{1}$$

In (1), $\alpha_{m,n}$ is an attenuation factor which accounts for the loss due to the scattering cross-section, the r^{-1} propagation loss, as well as other losses such as absorption and scattering from other obstacles in the propagation path. The time delay term $T_{m,n}$ is found from geometrical considerations and is given by,

$$T_{m,n} = \frac{n_o}{c}\left(R + nd_R \sin\theta_o - md_T \sin\theta_o\right), \quad m = 0, 1, \ldots, M-1, \quad n = 0, 1, \ldots, N-1 \tag{2}$$

where n_o is the refractive index of the intervening medium, here assumed constant and equal to unity, c is the speed of light in air, and d_T and d_R are the element spacing for the transmit and receive arrays, respectively. The distances from the $m = 0$ element of the transmitter array to the $n = 0$ element of the receive array is designated as R. It is assumed that the receiver and transmitting arrays are in the other's far-field for and that R a makes an angle θ_o with respect to the normal of the transmit array and receive arrays as shown.

Examination of Figure 1 and Equation (1) shows that the signal $x_m(t), m = 0, \ldots, M-1$, arrives at each receiver element location as $y_n(t), m = 0, \ldots, M-1$, with a unique time delay specified by Equation (2). This in turn suggests that there are possibly $M \cdot N$ unique conditions that may be used to accurately estimate the position of the array. It is such a multiplicative effect that we wish to exploit in this system.

2.2 Multi-Wavelength Diversity Beamsteering

The architecture of the MIMO-based optical transmit-receive employing wavelength diversity is shown in Figure 2. The transmitter portion of the system consists of *M* independent CW lasers, each operating a slightly different wavelength λ_m, where

$$\lambda_m = \lambda_o + m\Delta\lambda \tag{3}$$

Clearly the *M* independent laser sources will be mutually incoherent. Information is transmitted by modulating the intensity of each laser using an electrical-to-optical intensity modulator driven with the desired information. We can express the modulated laser signal transmitted by the m^{th} radiator with its complex representation, or,

$$x_m(t) = I_m \tilde{x}_m(t) e^{j\left(\frac{2\pi c}{\lambda_m}t + \varphi_m\right)}, m = 0, \ldots, M-1 \tag{4}$$

where I_m is the intensity of laser *m* with wavelength λ_m, and φ_m is an (unknown) phase associated with the m^{th} laser. Clearly for independent light sources the phase of any one laser is uncorrelated to that of any other laser. Since beamforming will be accomplished using time delay, not phase shift methods, the bandwidth of the modulating signals $\tilde{x}_m(t)$ will not impose any limitations on the overall system performance. It is assumed however that $\tilde{x}_m(t)$ is slowly-varying when viewed on an optical time scale. Each laser is fiber coupled to one element of a coherent fiber bundle which constitutes the radiating array of point sources. The use of a fiber bundle means that a potentially large number of transmitter elements are possible.

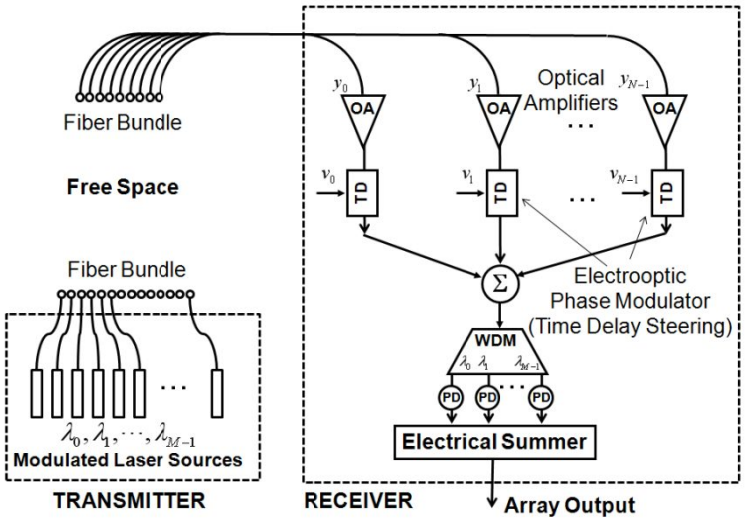

Figure 2: Multi-Wavelength MIMO beamforming architecture using *M* independent, incoherent modulated continuous wave (CW) laser sources of slightly differing wavelengths.

The receiver portion of the array consists of *N* optical fibers, again realized as a coherent fiber bundle, with the signal level boosted with an optical amplifier (OA). From Equation (1) it is seen that the signal at the n^{th} receive element includes all *M* wavelengths, and can be expressed as,

$$y_n(t) = \sum_{m=0}^{M-1} \tilde{x}_m\left(t - T_{m,n}\right) e^{j\frac{2\pi c}{\lambda_m}\left(t - T_{m,n}\right)} e^{j\varphi_m} \tag{5}$$

In Equation (5) it is assumed that the intensity I_m of each laser is identical, namely, $I_m = I_o, m = 0, \ldots, M-1$, and that the scattering/attenuation coefficient $\alpha_{m,n}$ is also identical for all values of *m* and *n*, and have been normalized to unity.

Referring again to Figure 2, the received signal $y_n(t)$ is delayed by time $T_{PM}(n)$ using a time delay unit (TD), perhaps an electrooptic phase modulator, with the amount of delay controlled via the applied voltage v_n. The corresponding delayed version of $y_n(t)$ is,

$$y_n\left[t-T_{PM}(n)\right]=\sum_{m=0}^{M-1}\tilde{x}_m\left(t-T_{m,n}-T_{PM}(n)\right)e^{j\frac{2\pi c}{\lambda_m}\left(t-T_{m,n}-T_{PM}(n)\right)}e^{j\varphi_m} \tag{6}$$

An important consideration for this architecture concerns the ability of a commercial electrooptic phase modulator to provide the necessary amount of time delay needed to electronically steer the array aperture. To address this concern, consider that an *N*-element uniform linear array with element spacing *d* would require a maximum time delay of $\pm(N-1)\frac{n_o d}{c}$ to steer the aperture by $\pm 90°$. But since the element spacing here is small (typically a hundred wavelengths, with the wavelengths on the order of a micron), a simple calculation shows that the maximum time delay required is on the order of hundreds of femtoseconds. Time delay on this order is obtainable, in principle, from a commercially available device such as a Lithium Niobate electrooptic phase shifter.

Since the modulating signal $\tilde{x}_m(t)$ is narrowband when compared with its optical carrier, and since $T_{PM}(n) \ll T_{m,n} \approx \frac{n_o}{c}R$, the argument in Equation (6) is well-approximated by

$$\tilde{x}_m\left(t-T_{m,n}-T_{PM}(n)\right)\approx\tilde{x}_m\left(t-\frac{n_o}{c}\left(R_R+R_T\right)\right)=x_m \tag{7}$$

and so Equation (6) may be written,

$$y_n\left(t-T_{PM}(n)\right)=\sum_{m=0}^{M-1}x_m e^{j\frac{2\pi c}{\lambda_m}\left(t-T_T(m)-T_R(n)-T_{PM}(n)\right)}e^{j\varphi_m} \tag{8}$$

As shown in Figure 3 the delayed signals $y_n\left(t-T_{PM}\right)$ are summed (optically) using an equal path-length summer such as a 1 x *N* coupler. Though not shown explicitly in Figure 3, each of the fibers (waveguides) at the summer inputs must have a means of equalizing the path length. For example, this can be accomplished using a variable retro-reflecting prism for a coarse delay adjustment and an additional electrooptic phase modulator for fine adjustment. These delays are used solely for path-length equalization and are not used for beam steering. Ideally these delays, once set, would require further adjustment to only compensate for any long-term drift. Making use of Equation (2) the output of the summer can be written as,

$$y_S(t)=\sum_{n=0}^{N-1}\sum_{m=0}^{M-1}x_m e^{j\frac{2\pi c}{\lambda_m}\left(t-T_{m,n}(m)-T_{PM}(n)\right)}e^{j\varphi_m}=\sum_{m=0}^{M-1}x_m e^{j\frac{2\pi c}{\lambda_m}\left(t-\frac{n_o}{c}\left(R-md_T\sin\theta_o\right)\right)}e^{j\varphi_m}\sum_{n=0}^{N-1}e^{-jn_o\frac{2\pi}{\lambda_m}\left(nd_R\sin\theta_o+T_{PM}(n)\right)} \tag{9}$$

Equation (9) suggests that we choose $T_{PM}(n)=-n\,n_o d_R\sin\theta$, where θ represents the desired steer angle. Noting that the second sum on the right-hand-side of (9) can be expressed in closed form, Equation (9) becomes,

$$y_S(t)=\sum_{m=0}^{M-1}x_m c_m(\theta,\theta_o)e^{j\frac{2\pi c}{\lambda_m}\left(t-\frac{n_o}{c}\left(R-md_T\sin\theta_o\right)\right)}e^{j\varphi_m} \tag{10}$$

where

$$c_m(\theta,\theta_o)=e^{-j\frac{N-1}{2}\frac{2\pi n_o}{\lambda_m}d_R\left(\sin\theta_o-\sin\theta\right)}\frac{\sin\left(N\frac{\pi n_o}{\lambda_m}d_R\left(\sin\theta_o-\sin\theta\right)\right)}{\sin\left(\frac{\pi n_o}{\lambda_m}d_R\left(\sin\theta_o-\sin\theta\right)\right)} \tag{11}$$

Equation (11) clearly reveals that the beam characteristics are a function of wavelength λ_m, a characteristic that will be used to great advantage in the analysis that follows. The output of the summing device is then

directed to a wavelength demultiplexer (WDM in Figure 3), realized, for example, using an arrayed waveguide grating device, which separates the individual wavelength components of the summed signal. The output of the $m^{\underline{\text{th}}}$ WDM (corresponding to λ_m) is,

$$y_{WDM_m}(t) = x_m c_m(\theta,\theta_o) e^{j\frac{2\pi c}{\lambda_m}\left(t-\frac{n_o}{c}(R-md_T\sin\theta_o)\right)} e^{j\varphi_m} \tag{12}$$

where an ideal, unit amplitude rectangular bandpass transmission characteristic for the WDM has been assumed.

Each of the $y_{WDM_m}(t), m = 0,\ldots M-1$ signals are now detected using *M* high-speed photodiodes, and these detected electrical signals can be written as

$$y_{WDM_m}(t) = x_m \left|c_m(\theta,\theta_o)\right| \tag{13}$$

The electrical detection process strips off any optical phase. This eliminates the random phase term associated with each laser as well as any phase associated with the propagation delay from the transmitter to the receive element. This in turn shows that the WDM output is not a function of the transmitter aray spacing. Equation (13) also shows that the $m^{\underline{\text{th}}}$ WDM output consists of the $m^{\underline{\text{th}}}$ modulating signal x_m weighted by the angular dependent factor $\left|c_m(\theta,\theta_o)\right|$. This weighting function $\left|c_m(\theta,\theta_o)\right|$ is simply the array factor of an *N*-element uniform linear array with element spacing d_R. A careful examination of Equation (9) reveals two important features of the multi-wavelength approach; the first is that the main lobe occurs when $\theta = \theta_o$ for all wavelengths λ_m as expected for a time-steered array. The second feature is that since $d_R \gg \frac{\lambda_m}{2}$, many grating lobes will be present, but unlike the main lobe, the angular location of the grating lobes varies with wavelength. Specifically, grating lobes occur when $\sin\left(\frac{\pi n_o}{\lambda_m} d_R(\sin\theta_o - \sin\theta_G)\right) = 0$ or when $\frac{\pi n_o}{\lambda_m} d_R(\sin\theta_o - \sin\theta_G) = p\pi$ where *p* is an integer. Solving for the position θ_G of the grating we find,

$$\theta_G = \arcsin\left(\sin\theta_o - p\frac{\lambda_m}{n_o d_R}\right), \quad p = 1,\ldots,\left\lfloor\frac{\lambda_m}{n_o d_R}\right\rfloor \tag{14}$$

where $\left\lfloor\frac{\lambda_m}{n_o d_R}\right\rfloor$ is the largest integer less than $\frac{\lambda_m}{n_o d_R}$. This property of an array factor, namely that main beam that is fixed in location while grating lobes (and null locations) vary with wavelength has been previously used to implement a broadband RF beamforming system with steerable broadband nulls [10, 11]. As will be subsequently shown, this diversity in the location of the grating lobes/null positions as a function of the wavelength is what allows for the design of a high-resolution electronically scanned array.

Referring again to Figure (2), each detected WDM output is now summed using an equal path length electrical summer. This gives the final array output as,

$$y(t) = \sum_{m=1}^{M-1} y_{WDM_m}(t) = \sum_{m=1}^{M-1} x_m \left|c_m(\theta,\theta_o)\right| \le x_{m,\max} \sum_{m=1}^{M-1} \left|c_m(\theta,\theta_o)\right| \tag{15}$$

Where $x_{m,\max}$ is the maximum amplitude of x_m. Further note that the sum in (15) will add maximally only for $\theta = \theta_o$. This is easily seen by examination of Figure (3), which illustrates the magnitude of $c_m(\theta)$ for $m = 0,\ldots,9$, as a function of the parameter (angle) θ. For clarity Figure 3 shows a "zoomed-in" portion of the angular spectrum that includes the main beam along with the first grating lobe. It is seen how

the main beam is always scanned to the same chosen angle (20° in this example) regardless of laser wavelength, while the grating lobes differ in location by a slight amount.

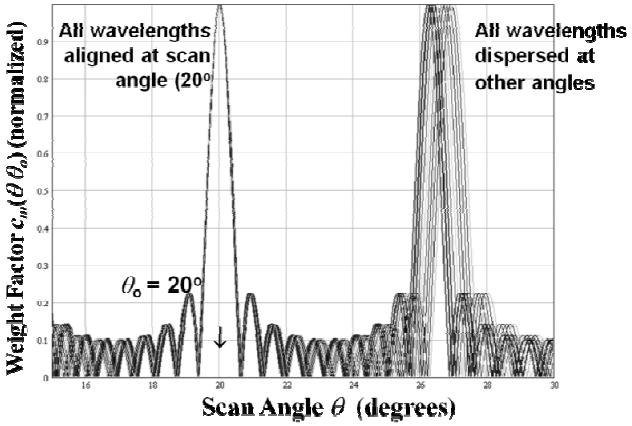

Figure 3: Unit-normalized weight coefficient $|c_m|$ vs. angular spectrum with the laser wavelength as a parameter. The figure shows only the portion of the angular spectrum containing the main beam and the first grating lobe.

3 ANTICIPATED PERFORMANCE

3.1 Numerical Simulation

To illustrate the expected performance of the multi-wavelength MIMO approach for laser radar applications, a numerical simulation is provided. Consider then a system with the following specifications:

Table 1: Multi-Wavelength MIMO System Parameters	
Number of Transmit Lasers	$M = 100$
Number of Receive Fibers	$N = 100$
Minimum Wavelength	$\lambda_o = 1.5\ microns$
Frequency Increment	$\Delta f = 50\ \mathrm{GHz}$
Receiver Fiber Element Spacing	$d_R = 60\lambda_o$
Steering Location	$\theta_o = 20°$

Figure 4 shows the resultant normalized array output transfer function analytically expressed by (15). Specifically, the plot on the left in Figure 4 shows the result for a of steer angle of $\theta_o = 20°$. For the clarity the plots on the right in Figure 4 expands the axis to show the detailed character of the main beam and compares the result with that for a traditional $N\times M$-element uniform linear array. All results have been unit-normalized to aid in the comparison.

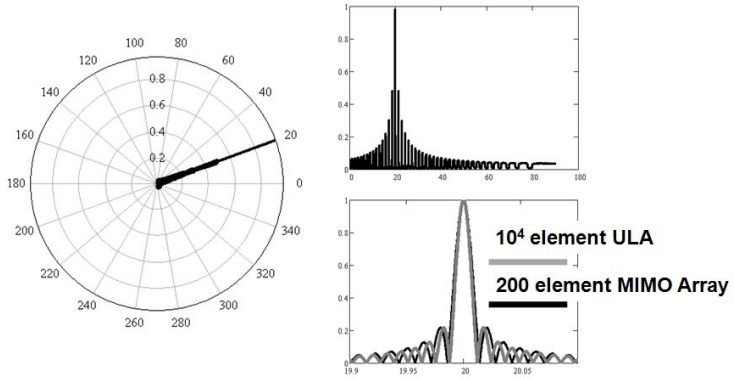

Figure 4: Simulated response for an ten-element transmit, ten-element receive MIMO laser radar. The plot on the left shows the effective radiation pattern steered to an angle of 20°. The plot on the top right shows the sibelobe lenes while the plot on the lower right compares the beamwidth for the 20° MIMO array pattern with that of a 100×100-element Uniform Linear Array (ULA).

4 CONCLUSIONS

4.1 Summary

The analysis presented and illustrated by simulation shows that even for arrays with element spacing greater that the usual half-wavelength, significant advantages are realized. First, as expected, the directional gain on-target is increased by a factor of $M \cdot N$ while using only M lasers. Secondly it is seen that the beamwidth that of a $M \cdot N$ - element array. For a receiver element spacing exceeding $40\lambda_o$, which, under normal circumstances would produce many grating lobes, produces only one main beam. The diversity approach utilized here, namely the use multiple laser wavelengths, results in a significant amplitude reduction at all angles except that of the main lobe. Tradeoffs among the various system parameters would produce a design that has been optimized for a particular interconnect application.

5 REFERENCES

[1] H. Zmuda and E.N. Toughlian, Photonic Aspects of Modern Radar, Boston, *Artech House*, 1994.

[2] P.F. McManamon, T.A. Dorschner, D.L. Corkum, L.**J.** Friedman, D.**S.** Hobbs, M. Holz, S. Liberman, H.Q. Nguyen, D.P. Resler, R.C. Sharp, and E.A. Watson, "Optical Phased Array Technology," *Proceedings Of The IEEE*, Vol. 84, No. 2, February 1996, pp. 268-298.

[3] N.A. Riza, Editor, Selected Papers on Photonic Control Systems for Phased Array Antennas, SPIE Milestone Series Volume MS 136, Bellingham, Washington: SPIE Optical Engineering Press, 1997

[4] I. Bekkerman and J. Tabrikian, "Spatially coded signal model for active arrays," *The 2004 IEEE International Conference on Acoustics, Speech, and Signal Processing*, Montreal, Quebec, Canada, vol. 2, pp. ii/209–ii/212, March 2004.

[5] J. Li and P. Stoica, "MIMO radar – diversity means superiority," *The Fourteenth Annual Workshop on Adaptive Sensor Array Processing*, MIT Lincoln Laboratory, Lexington, MA, June 2006.

[6] L. Xu, J. Li, and P. Stoica, "Adaptive techniques for MIMO radar," *4th IEEE Workshop on Sensor Array and Multi-channel Processing*, Waltham, MA, July 2006.

[7] L. Xu, J. Li, and P. Stoica, "Radar imaging via adaptive MIMO techniques," *14th European Signal Processing Conference*, (invited), Florence, Italy, September 2006. (available on the website: ftp://www.sal.ufl.edu/xuluzhou/EUSIPCO2006.pdf).

[8] P. Stoica, J. Li, and Y. Xie, "On probing signal design for MIMO radar," to appear in *IEEE Transactions on Signal Processing*.

[9] N. Levenon, "Noncoherent Pulse Compression", *IEEE Transactions on Aerospace and Electronic Systems*, Vol. 42, No. 2, April 2006, pp. 756-765.

[10] H. Zmuda, E.N. Toughlian, M.A. Jones, P.M. Payson, "*Photonic Architecture for Broadband Adaptive Nulling with Linear and Conformal Phased Array Antennas*", Fiber and Integrated Optics, vol. 19, no. 2, March 2000, pp. 137- 154.

[11] H. Zmuda, E.N. Toughlian, P. Payson, and H. Klumpe, III, "*A Photonic Implementation of a Wideband Nulling System for Phased Arrays*", IEEE Photonics Technology Letters, Vol. 10, No. 5, pp. 725-727, May 1998.